Spiral Optical Fiber Sensor for Precision Vibration and Structural Strain Detection

Description

This study presents the design and theoretical analysis of a distributed fiber-optic sensing system for localization of mechanical vibrations and micro-strain in structural materials. The proposed architecture combines multimode and spiral single-mode optical fibers with different effective optical path lengths, enabling detection and spatial reconstruction of localized perturbations through differential signal propagation and timing analysis.

The sensing principle is based on strain-induced variations in optical propagation conditions, scattering losses, and signal delay between coupled optical channels. The spiral geometry increases the effective optical path length and enhances sensitivity to local deformations, while the use of multiple sensing lines improves robustness in the presence of simultaneous perturbations.

The proposed configuration represents a compact and scalable sensing approach that may be integrated into aerospace structures, industrial systems, seismic monitoring networks, and laboratory-scale experimental platforms. Analytical estimates indicate that the system is capable of resolving localized structural perturbations with high spatial sensitivity under realistic assumptions regarding timing resolution and optical losses.

Introduction

Optical losses in bent fiber-optic waveguides arise from partial disruption of total internal reflection under local deformation conditions (Figure 1). Such bending-induced scattering produces detectable optical leakage, the intensity of which depends on the local curvature and structural perturbation of the fiber.

Figure 1

This effect can be utilized for localization of mechanical vibrations and micro-strain in distributed sensing systems. In the proposed configuration, a multimode optical fiber is used as the primary sensing channel in order to enhance sensitivity to bending-induced scattering.

A single-mode fiber helically wound around the multimode channel serves as an auxiliary propagation path for the scattered optical signal. Radiation escaping from the multimode fiber may couple into the single-mode fiber and subsequently propagate in both longitudinal directions.

Because the effective optical path length of the spiral single-mode channel differs from that of the direct multimode channel, the time delay between signal registrations can be used to reconstruct the coordinate of the perturbation along the cable.

Sensor Configuration

Mechanical vibrations of an optical fiber integrated into a structural element lead to variations in the optical path length and to perturbations of the internal reflection conditions of the guided radiation (see Figure 2).

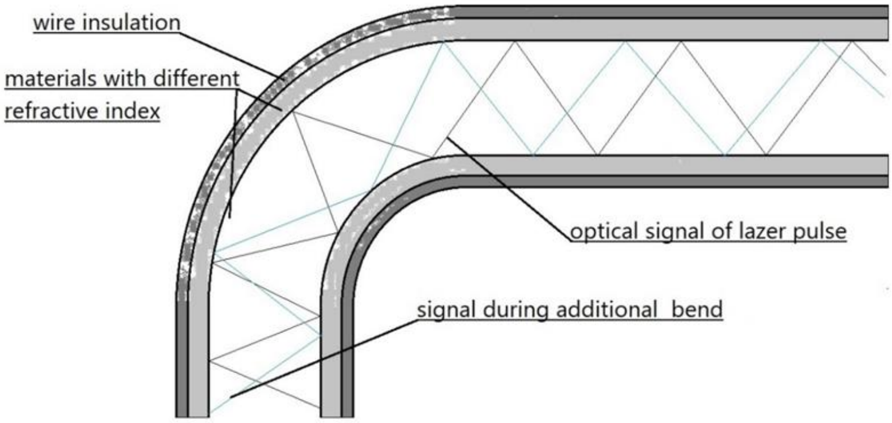

Figure 2 Optical losses induced by local bending of the fiber

The sensing cable consists of two optical fibers arranged within a common braid: a multimode fiber (MMF) and a single-mode fiber (SMF). The single-mode fiber is helically wound around the multimode fiber, forming a composite structure with different effective optical path lengths for signal propagation (see Figure 3).

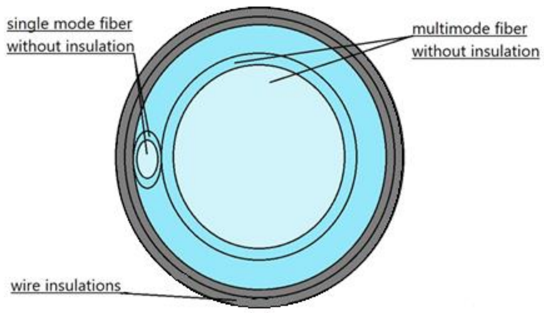

Figure 3

The radiation source is coupled to one end of the multimode fiber, while the opposite end is connected to receiver 1. The single-mode spiral fiber is connected, at the source side, to a photodetector via a partially reflective optical element. At the opposite end, it is connected to receiver 2, as shown in Figure 4. The receivers and the photodetector convert the optical signals into electrical signals for further processing.

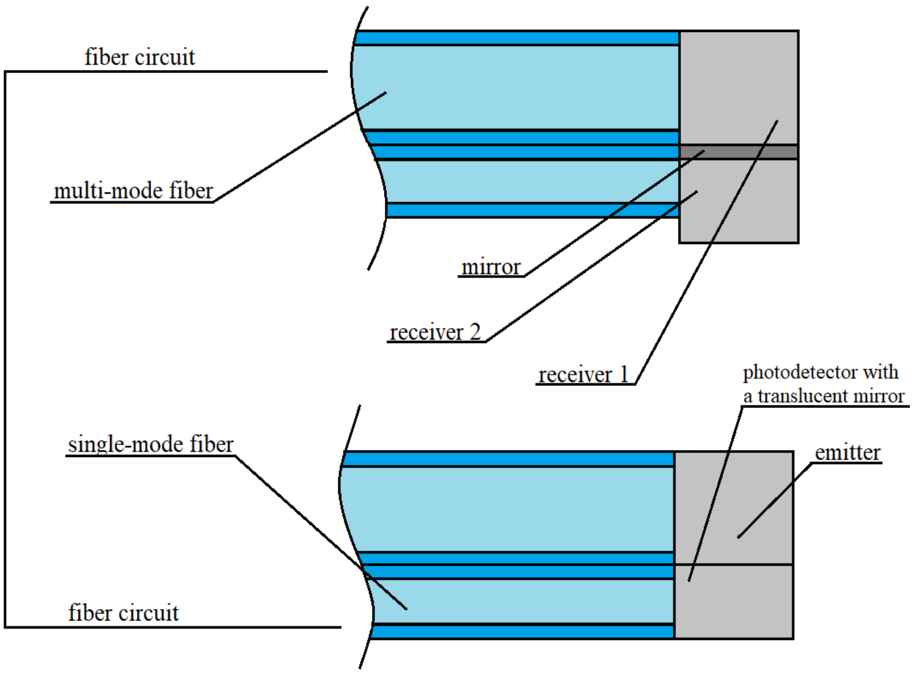

Figure 4. Optical sensing system layout

The receiver unit in the single-mode channel includes a photodetector and an optical element (e.g., a mirror or a metamaterial membrane) configured to reflect incident radiation at non-normal incidence angles, enabling controlled signal routing and detection (see Figure 5).

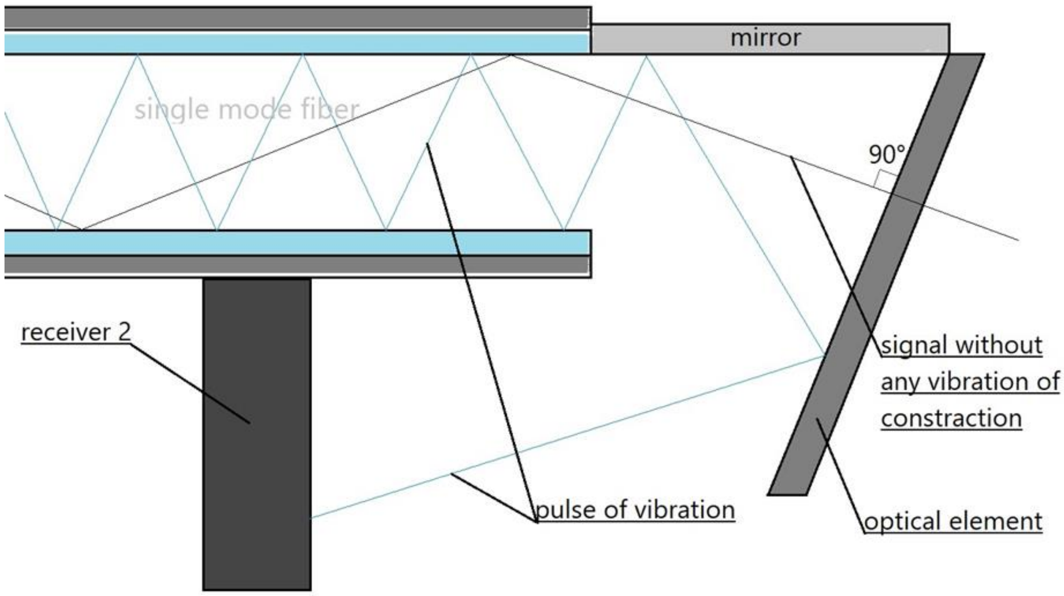

Figure 5. Single-mode receiver unit

This configuration enables differential signal timing and phase analysis for localization of perturbations along the sensing line.

During the initial calibration stage, the optical system is adjusted such that the radiation exiting the single-mode channel is incident normally on the optical element and is fully absorbed. Under these conditions, receiver 1 registers no signal, while receiver 2 records a stationary baseline response corresponding to the steady-state optical losses and intrinsic geometric configuration of the fiber.

In the nominal operating regime, structural vibrations induce a reproducible modulation of the optical signals in both channels due to strain-induced variations in optical path length and scattering losses. The corresponding temporal characteristics are recorded and stored as a reference state.

Deviations from the reference signals $S_1(t)$ and $S_2(t)$, representing the temporal responses of receiver 1 (MMF channel) and receiver 2 (SMF channel), respectively, are interpreted as indicators of anomalous structural perturbations. Due to the difference in effective optical path lengths, signals originating from the same perturbation arrive at the receivers with a time delay Δt, which is used for spatial localization.

The coordinate of the perturbation is reconstructed from the measured delay Δt using the analytical expressions derived in Section Calculation for the relationship between time delay and spatial position.

In the presence of multiple simultaneous perturbations, the received signals may form ambiguous pairs. To resolve this ambiguity, both forward and reverse propagation paths in the spiral channel are utilized, yielding a system of two independent equations for each candidate signal pair. Only those pairs for which the system admits a consistent (physically admissible) solution are considered valid.

The scattered radiation generated at a local deformation point propagates in both directions along the single-mode fiber. Although the exact distribution depends on geometric and modal parameters, it is assumed to be approximately symmetric on average for the purpose of statistical signal reconstruction.

The signal processing procedure is implemented as an adaptive algorithm (see Figure 6) that performs dynamic pairing of detected events and evaluates candidate solutions based on consistency criteria.

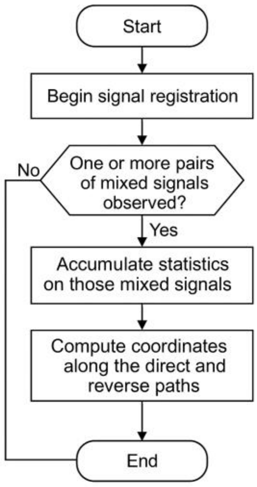

Figure 6

The implementation of the described sensing and processing principles imposes specific constraints on the physical design of the cable. In practice, the system is realized for predefined cable lengths, each associated with a specific set of calibration constants, including the effective propagation velocity of light in the fiber, the spiral pitch, and the refractive indices of the optical media.

Since the minimum bending radius of a single-mode fiber is significantly larger than that of a multimode fiber, the cable design incorporates a compliant core that preserves flexibility while maintaining geometric stability. The radius of the core is selected to be comparable to the minimum bending radius of the single-mode fiber. For example, fibers of the G.657 standard exhibit minimum bend radii ranging from approximately 5 mm to 10 mm depending on the subclass.

Multimode fibers are arranged around the core in a single-layer configuration, forming the primary sensing channel. A single-mode fiber is then helically wound around this structure, providing a secondary channel with an increased effective optical path length. The insulation layer provides both optical isolation and mechanical protection while maintaining sufficient flexibility to preserve sensitivity to structural vibrations. The mechanical integrity of the core and insulation is critical, as variations in the spiral pitch may introduce systematic errors in the localization of perturbations.

The described configuration ensures the mechanical compliance and optical sensitivity required for reliable detection and localization of structural perturbations in complex engineering systems.

Analytical Model

Based on the minimum bending radius of a single-mode fiber, we assume for preliminary calculation the radius of the core with an environment of multimode fiber equal to 5 millimeters. Since the outer diameter of a standard optical fiber is 125 micrometers, the diameter of the core itself will be 9.750 millimeters.

Since the single-mode fiber is wound on a core with a multimode without gaps, the spiral pitch will be a multiple of the outer diameter of the fiber, i.e. 125 micrometers. Let's take the number of single-mode fibers equal to 48. Then the spiral pitch is 48*0.125 = 6.0 millimeters.

Spiral pitch (along the multimode fiber axis): 6 mm;
Multimode fiber diameter (without insulation): 125 μm;

The formula for the length of a cylindrical spiral in one step:

$$l = \sqrt{(2\pi r)^2 + h^2},$$

where:
h = 6.0 mm – pitch of spiral;
r = 5.0 mm - radius;

$$l = \sqrt{(2\pi \cdot 0.005)^2 + (0.006)^2} \approx 0{,}032 \text{ m};$$

This means that for every 6 mm along the axis (multi-mode fiber), there is ≈ 32 mm of single-mode fiber.

$$x/x' = h/l,$$

$$x/x' = 3/16 = 0.1875,$$

where x/x' - the ratio of the lengths of a multi-mode fiber to a single-mode fiber in a cable section from the coordinate of the detected vibration to one of the cable ends.

Now let's calculate the signal travel time over a 20-meter-long cable. The speed of light in a fiber:

$$V = c/n,$$

where:
n - refractive indices of the fiber core;
c – speed of light in absolute vacuum.
Time of passage over multimode optical fiber, taking into account pulse dispersion:

$$t = (L \cdot n_m)/c + \Delta t_{modal},$$

$$\Delta t_{modal} \approx (L \cdot n_m)/c \cdot \Delta/2,$$

where:

n_m - refractive index of multi-mode fiber: ≈ 1.48 - typical for quartz fiber;
Δ - the relative difference in the refractive indices of the fiber core and cladding, let's take the value for standard multimode fibers ≈ 0.01;
L = 20 m. - sensing system length.

The formula for relative difference in the refractive indices:

$$\Delta = (n^2_{core} - n^2_{clad})/2n^2_{core};$$

$$t_1 = (20 \cdot 1.48)/3 \cdot 10^8 + (20 \cdot 1.48 \cdot 0.01)/2 \cdot 3 \cdot 10^8 \approx 9.916 \cdot 10^{-8}\ s = 99.16\ ns;$$

Time of passage over spiral single-mode optical fiber:

$$t = (L \cdot l \cdot n_s)/(c \cdot h),$$

where n_s - refractive index of single-mode fiber: ≈ 1.468 (typical for quartz fiber at 1.550):

$$t_2 = (20 \cdot 0.032 \cdot 1.468)/(0.006 \cdot 3 \cdot 10^8) \approx 52.196 \cdot 10^{-8}\ s = 521.96\ ns;$$

Time difference (delay):

$$\Delta t \approx 422.80\ ns.$$

Now we will derive the equation for finding the coordinate from the time difference between the movement of the signal along different paths, taking into account the main corrections:

$$t_1 = x \cdot n_m/c + x \cdot n_m \cdot \Delta/2c,$$

$$t_2 = 16x \cdot n_s/3c,$$

$$\Delta t = 16x \cdot n_s/3c - (x \cdot n_m/c + x \cdot n_m \cdot \Delta/2c),$$

$$\Delta t = (32x \cdot n_s - 6x \cdot n_m - 3x \cdot n_m \cdot \Delta)/6c,$$

$$\Delta x_1 = (\Delta t \cdot 6c)/(32n_s - 6n_m - 3n_m \cdot \Delta);$$

The same equation is corrected for the case when the signal propagates in the opposite direction along the spiral fiber:

$$t_2 = (2L-x)/V_s,$$

$$t_1 = x \cdot n_m/c + x \cdot n_m \cdot \Delta/2c;$$

$$t_2 = 16(2L-x) \cdot n_s/3c,$$

$$\Delta t = 32L \cdot n_s/3c - 16x \cdot n_s/3c - (x \cdot n_m/c + x \cdot n_m \cdot \Delta/2c),$$

$$\Delta x_2 = (32L \cdot n_s/3c - \Delta t) \cdot 6c/(6n_m + 3n_m \cdot \Delta + 32n_s);$$

In the case of mixed pairs of signals from different vibration points, the controller solves both equations in one system for all possible combinations of pairs:

$$\Delta x_1 = (\Delta t \cdot 6c)/(32n_s - 6n_m - 3n_m \cdot \Delta),$$

$$\Delta x_2 = (32L \cdot n_s/3c - \Delta t) \cdot 6c/(6n_m + 3n_m \cdot \Delta + 32n_s).$$

Only those pairs out of all possible pairs for which this system is solvable are a pair of signals from one vibration point. In this case, having a solution to a system of equations means that both equations individually have the same solutions for the same pair of signals.

Now, let's calculate the accuracy of the localization of the vibration point based on the difference in the signal travel time. Assuming a timing resolution in the picosecond range ($\delta t \sim 10^{-12}$ sec), which is achievable in modern photonic detection systems using high-speed photodetectors and time-to-digital conversion electronics, the theoretical localization accuracy can be estimated as:

$$\Delta x_1 = (\Delta t \cdot 6c)/(32n_s - 6n_m - 3n_m \cdot \Delta),$$

$$\delta(\Delta x_1)/\delta t = 6c/(32n_s - 6n_m - 3n_m \cdot \Delta),$$

$$\delta x_1 = (10^{-12} \cdot 6 \cdot 3 \cdot 10^8)/(32 \cdot 1.468 - 6 \cdot 1.48 - 3 \cdot 1.48 \cdot 0.01) \approx \mathbf{0.047 \times 10^{-3}\ m};$$

Calculation of accuracy according to the signal of a single-mode fiber going in the opposite direction:

$$\Delta x_2 = (32L \cdot n_s/3c - \Delta t) \cdot 6c/(6n_m + 3n_m \cdot \Delta + 32n_s),$$

$$\delta(\Delta x_2)/\delta t = -6c/(6n_m + 3n_m \cdot \Delta + 32n_s),$$

$$|\delta(\Delta x_2)| = 6c \cdot \delta t/(6n_m + 3n_m \cdot \Delta + 32n_s),$$

$$|\delta(\Delta x_2)| = 6 \cdot 3 \cdot 10^8 \cdot 10^{-12}/(6 \cdot 1.48 + 3 \cdot 1.48 \cdot 0.01 + 32 \cdot 1.468) \approx \mathbf{0.032 \times 10^{-3}\ m};$$

Since the two accuracy lines differ, we take the maximum value from them: **0.047×10^{-3} m.**

To calculate the entangled pairs of signals, you can use two such systems connected to a common controller in parallel, but without calculating the time for the signal reflected from the mirror. Both cables must be tightly clamped in a common braid of optical fibers of the same standard.

Let h_1 and h_2 denote the spiral pitches of the first and second sensing lines, respectively. To avoid degeneracy of the coordinate solutions, it is required that $h_1 \neq h_2$. The resulting difference in propagation-delay functions provides an independent localization criterion for identifying signal pairs originating from the same vibration point.

Then, in the case of several vibration locations, the controller program finds a solution to two equations of the same type for two pairs of signals, sorting through all possible pairs of signals. The pair of signals for which the solutions of the two equations coincide is a pair of signals from the same location of extraneous vibrations. Since pairs of signals are duplicated at different time intervals between the signals in the pair, the correspondence is uniquely identified.

The controller calculates only those signals that go in the forward direction, the photodetector in the opposite direction sends messages to the controller about the reverse signals and they are not processed.

let's calculate the parameters of the second cable by taking the spiral pitch h' value of 60 millimeters:

$$l' = \sqrt{(2\pi r)^2 + h'^2},$$

$$l' = \sqrt{(2\pi \cdot 0.005)^2 + (0.06)^2} \approx 0{,}068 \text{ m};$$

This means that for every 60 mm along the axis (multi-mode fiber), there is ≈ 68 mm of single-mode fiber:

$$h'/l' \approx 0.882;$$

Time intervals and equation for coordinate:

$$t_1 = t'_1 = x_2 \cdot n_m/c + x_2 \cdot n_m \cdot \Delta/2c,$$

$$t_2 = 16x_2 \cdot n_s/3c,$$

$$t'_2 = 34x_2 \cdot n_s/3c,$$

$$\Delta t' = 17\Delta x_2 \cdot n_s/15c - (\Delta x_2 \cdot n_m/c + \Delta x_2 \cdot n_m \cdot \Delta/2c),$$

$$\Delta t' = \Delta x_2 \cdot (34n_s - 30n_m - 15n_m \cdot \Delta)/30c,$$

$$\Delta x_2 = (\Delta t' \cdot 30c)/(34n_s - 30n_m - 15n_m \cdot \Delta);$$

Calculation of accuracy for second line:

$$\delta x_2 = (10^{-12} \cdot 30 \cdot 3 \cdot 10^8)/(34 \cdot 1.468 - 30 \cdot 1.48 - 15 \cdot 1.48 \cdot 0.01) \approx \mathbf{1.74 \times 10^{-3}\ m};$$

For the case of mixed pairs of signals from different vibration points:

$$\Delta x_1 = (\Delta t \cdot 6c)/(32n_s - 6n_m - 3n_m \cdot \Delta),$$

$$\Delta x_2 = (\Delta t' \cdot 30c)/(34n_s - 6n_m - 3n_m \cdot \Delta).$$

In practical fiber-based sensing systems, the effective accuracy may be limited by detector jitter, modal dispersion, thermal drift, optical losses, and signal-to-noise ratio. Therefore, to take into account the accuracy of the sensor, we take the value

$\Delta t \sim 10^{-11}$ sec. Since the two accuracy lines differ, we take the maximum value from them: $\mathbf{1.74 \times 10^{-2}}$ **m**.

The localization sensitivity depends on the ratio between the spiral and axial propagation lengths. Increasing the optical path difference between the multimode and single-mode channels improves timing sensitivity, whereas excessively large spiral pitches reduce the differential delay and therefore decrease localization accuracy.

A trade-off exists between localization sensitivity and signal-pair discrimination. The first sensing line should therefore employ a minimal spiral pitch to maximize timing sensitivity, whereas the second line should use a different, larger pitch chosen such that the resulting localization error remains within acceptable limits while still providing an independent localization criterion.

The intensity of the optical pulse coupled into the single-mode fiber is expected to depend on the local bending amplitude of the composite cable structure and, in particular, on deformation of the multimode fiber. Under fixed installation and calibration conditions, the corresponding transfer relation can be experimentally determined during the initial system setup.

Consequently, the amplitude of anomalous vibrations may be estimated from the intensity of the optical signal detected in the single-mode channel by the photodetector and receiver subsystem.

The bending radius of the spiral single-mode fiber is defined by the cable geometry and can be treated as a fixed system parameter. In contrast, the bending radius of the multimode fiber varies with the instantaneous deformation of the entire cable during vibration. Therefore, the signal amplitude detected in the single-mode channel is primarily governed by bending-induced scattering in the multimode fiber, while the spiral single-mode winding provides a calibrated distributed capture efficiency. Under this approximation, the detected amplitude may be written as:

$$P_{SMF}(t) \propto P_{MMF}(R_C(t)) \cdot \eta_{SMF}(R_{SMF,0}),$$

where:
$P_{SMF}(t)$ is detected optical intensity;
$R_C(t)$ is the instantaneous bending radius of the composite cable;
$R_{SMF,0}$ is the fixed bending radius of the spiral single-mode fiber;
$P_{MMF}(R_C(t))$ is the bending-induced scattered optical power generated in the multimode fiber;
$\eta_{SMF}(R_{SM,0})$ is the effective distributed capture efficiency of the spiral single-mode channel.

Parallel distributed sensor lines may provide an additional correlation criterion based on relative pulse intensity maxima, improving identification of mixed or partially overlapping signal pairs during simultaneous perturbation events.

If extended toward interferometric operation, the proposed sensing architecture could potentially provide sensitivity to extremely small variations in effective optical path length through differential phase measurements. In this respect, the concept bears a distant analogy to large-scale interferometric systems such as

LIGO, where differential optical-path variations are used to detect strain-like perturbations [1, Ch. 19]:

$$\Delta\phi = (2\pi/\lambda) \cdot \Delta L,$$

where ΔL - effective optical path variation.

Such an approach could, in principle, be investigated as a possible method for probing extremely weak effective metric-like perturbations or distributed optical-path distortions in structured field environments.

In such a configuration, intensity-based measurements could provide localization and deformation amplitude estimates, while interferometric phase analysis could extend the sensitivity of the system toward extremely small distributed optical-path perturbations.

Conclusion

The proposed dual-channel fiber-optic sensing architecture enables localization of structural perturbations through differential signal propagation in multimode and spiral single-mode fibers. The analytical model demonstrates that the use of multiple sensing lines with different effective optical path lengths improves the robustness of signal pairing and reduces ambiguity in the presence of simultaneous perturbations.

The second localization approach, based on parallel sensing lines with different spiral geometries, provides improved spatial resolution and eliminates the need for long-term statistical accumulation of signal correlations. At the same time, the original forward/reverse propagation method may remain useful as a redundant operating mode in the event of partial cable degradation or signal loss.

The analysis further indicates that localization accuracy strongly depends on timing resolution, spiral geometry, modal dispersion, and optical losses. Increasing the effective optical path difference between sensing channels improves coordinate reconstruction accuracy, while excessive multimode scattering may reduce performance at large distances.

The proposed sensing principle may also be generalized to alternative architectures, including hybrid photonic–electronic detection schemes in which optical scattering events are converted directly into electrical signals. Such approaches could simplify signal processing and improve integration with distributed monitoring systems.

Owing to its distributed nature and high sensitivity to localized perturbations, the proposed technology may find applications in structural health monitoring, industrial diagnostics, seismic sensing, and aerospace systems. Further work is required to evaluate experimental feasibility, optimize signal-processing algorithms, and characterize system performance under realistic operating conditions.

In principle, the proposed fiber-optic sensing approach may be extended toward interferometric configurations capable of detecting extremely small variations in effective optical path length. In this respect, the concept bears a distant analogy to large-scale interferometric systems such as LIGO, where differential path measurements are used to probe minute perturbations.

However, in the present implementation the sensor is primarily sensitive to structural deformations and environmental influences, which are expected to dominate over any potential metric effects. Therefore, such an analogy should be regarded as conceptual rather than operational.

[1] B. E. A. Saleh and M. C. Teich, Fundamentals of Photonics, 2nd ed., Wiley-Interscience, Hoboken, NJ (2007), ISBN: 978-0471358329.